Two-hole localization mechanism for electronic bond rupture of surface atoms by laser-induced valence excitation of semiconductors

K. Tanimura,[1] E. Inami,[1] J. Kanasaki,[1] and Wayne P. Hess[2]
[1]*The Institute of Scientific and Industrial Research, Osaka University, 8-1 Mihogaoka, Ibaraki, Osaka 567-0047, Japan*
[2]*Pacific Northwest National Laboratory, Richland, Washington 99352, USA*
(Received 25 December 2005; published 27 July 2006)

We examine the mechanism of electronic bond rupture on semiconductor surfaces induced by laser-generated nonequilibrium three-dimensional valence excitation associated with strong carrier diffusion. For such excited systems, the density of subsurface valence holes that contribute to two-hole localization on the surface is characterized by quasi-Fermi-levels and effective temperature. The rate of two-hole localization, formulated for equilibrated two-dimensional electronic systems by Sumi [Surf. Sci. **248**, 382 (1991)], is reformulated, and a simple analytical expression is yielded for moderate excitation densities. The resulting theoretical model has been successfully applied in the analysis of recent laser-induced atomic desorption experiments on InP and Si surfaces.

DOI: 10.1103/PhysRevB.74.035337 PACS number(s): 79.20.Ds, 61.80.Ba, 68.55.Ln, 61.72.Ji

I. INTRODUCTION

The surfaces of covalent semiconductors undergo drastic reconstructions, governed by the balance between the energy gained from variations in the bonding properties and the elastic energy lost due to distortions from ideal sp^3 bonding.[1] Reconstructed surfaces have electronic properties significantly different from those in bulk crystals and exhibit several surface-specific phenomena such as structural instability under electronic excitation. As demonstrated by several recent studies, laser excitation induces electronic bond rupture, which leads to drastic changes in semiconductor surface structure and desorption of constituent atoms.[2–12] The electronic process shows some important common features. First, atoms at perfect surface sites are subject to bond rupture,[2–8,10–12] thus demonstrating the intrinsic nature of the processes. Second, the desorbed species are ground-state neutral atoms; ions are not emitted. Third, the rate of bond rupture depends sensitively on the type of surface site and atomic species.[3,6,11,12] Finally, the rate of bond rupture shows superlinear dependence on the excitation laser intensity for photon energies between 1 and 4 eV.[6,7,9–12]

It is clear that charge redistribution on surfaces, induced by the generation and relaxation of surface excited states, plays a crucial role in the surface instability. Surface excited species can be populated by two different channels; direct surface-specific optical excitation, and indirect electronic excitation transfer from bulk to surface states. Since optical-transition energies between surface electronic states usually overlap those of bulk-electronic states, in most cases,[1] both channels can be active under excitation at a given photon energy. However, because of the small absorption coefficient of the surface,[13] most photoexcitation occurs in the bulk-valence system, where electron-hole pairs are generated with a high density. The dense valence excitation, typically 10^{19} cm^{-3}, can transfer to the surface electronic system through electron-phonon and/or electron-electron scattering,[14] leading to surface structural changes and a desorption of constituent atoms. In fact, recent results have shown clearly that bulk-valence excitation induces electronic bond rupture of surface atoms at intrinsic sites.[11,12] Therefore, quantitative examination of the effects of bulk-valence excitation on surface bond rupture is important for understanding the mechanism of this surface-specific phenomenon, and for developing methods to control electronic processes on surfaces.

Sumi modeled the effects of valence holes on semiconductor surface bond rupture, and found localization of two holes (two-hole localization, THL), at the same surface bond, to be important.[15] Although the two-hole (or multihole) mechanism has been widely used to describe ion desorption induced by core-hole excitation on ionic surfaces,[16,17] neutral and ion desorption mechanisms are obviously very different. The key assumption in the THL mechanism leading to neutral-atomic desorption (not ion desorption) is that surface bond rupture can be induced by strong lattice relaxations associated with a localization of two valence holes on the same surface bond.[15,18] This assumption is based on the Anderson negative U concept; that the localization of two carriers with the same charge is possible when strong lattice coupling results in favorable system energetics.[19] The negative U interaction of two-hole localized configurations corresponds to the displacement of surface atoms into the vacuum in the THL mechanism. Thus, together with the Coulomb interaction energy U and the valence bandwidth B, which are important to give an energy relationship in the two-hole mechanism for ion desorption,[16,17] the electron-lattice interaction S becomes a crucial physical quantity that characterizes the energy relationship in the THL mechanism.

One of the important predictions of Sumi's theory is a superquadratic dependence of the bond-rupture rate on the excitation density. The predicted superquadratic dependence, a result of quantum statistics of densely populated holes, has been verified experimentally for reconstructed Si surfaces and for III-V compound semiconductor surfaces.[6,7,9–12] Previous experimental results are at least qualitatively described by the THL mechanism. However, in the quantitative analysis of recent experimental results, we need to extend Sumi's formalism to the more general cases of valence excitation induced by laser irradiation, since Sumi formulated the rate

of successive localization of two holes on a surface bond only for a thermally equilibrated valence system.

For the thermally equilibrated system, the Fermi energy governs not only the hole distribution but also the transition rate of the second-hole localization step. Furthermore, the analytical THL rate expression becomes conventional for *equilibrated* valence holes confined two dimensionally to the surface region. However, laser-induced valence excitation is strongly nonequilibrium. For example, InP and GaAs(110)-(1×1) surfaces have no intrinsic surface states in the gap, and maintain flat-band conditions under excitation.[1] Recent surface carrier dynamics studies[20] indicate that *p*-type Si(001)-(1×1) also maintains a flat-band condition when excited. Under the flat-band condition, densely populated valence holes and conduction electrons, generated by laser excitation with photon energies larger than the band-gap energy, show strong nonequilibrium diffusion caused by a high concentration and temperature gradients. Therefore, instead of forming a system consisting of equilibrated two-dimensionally confined valence holes, nonequilibrium three-dimensional electron-hole pairs are generated by optical excitation.

The nonequilibrium features of valence holes may be more general for other semiconductor surfaces. The band bending of semiconductor surfaces may act to confine carriers in the near surface region. On surfaces of *n*-type crystals, upward band bending may form two-dimensionally confined valence holes at the weak-excitation limit. However, a finite band bending due to Fermi-level pinning can easily be reduced, due to the surface photovoltaic effect, to establish flat-band conditions under dense excitation.[1] Photoelectron spectroscopy studies have shown that the temporal change of the photovoltaic effect is very fast, and takes place within a few ps of excitation of Si surfaces.[21] The band, flattened under dense excitation, remains flat for microseconds.[22] Therefore, most photogenerated carries are governed by flat-band conditions shortly after ns-laser excitation and the valence excitation has a three-dimensional nonequilibrium character. The role of the nonequilibrium valence excitation is yet to be described theoretically and is the subject of this paper.

In this paper, we extend Sumi's THL model by incorporating results of previous theoretical studies of photoinduced electron-hole plasmas in semiconductors.[23,24] Under the assumption of a quasiequilibrium of the valence excitation, some quantitative expressions of Sumi's formulas are modified for nonequilibrium three-dimensional systems. Nonetheless, the essential conclusions of Sumi's theory remain unchanged. The extended theory is then applied successfully in the analysis of recent laser-induced desorption experiments on InP(110)-(1×1) and Si(111)-(2×1) surfaces.

II. THE RATE OF TWO-HOLE LOCALIZATION FOR NONEQUILIBRIUM VALENCE EXCITATION

A. Equation of particle balance for a three-dimensional plasma with carrier flow

Efficient carrier diffusion can dominate nonequilibrium dynamics of photogenerated electron-hole populations in semiconductors. Densely populated carrier dynamics has been investigated by Preston and van Driel in semiconductor laser annealing studies.[23,24] In their analysis, a quasiequilibrium was assumed, and quasi-Fermi-levels of electrons (ψ_e), holes (ψ_h), and an effective temperature T^* were used to describe local carrier distributions for temporal domains longer than a few ps.[23,24] Later studies of carrier dynamics on Si surfaces have confirmed that the electronic quasiequilibrium is established within 1 ps of fs-pulse excitation.[25,26] Then, under the effective-mass approximation, the quasiequilibrium local carrier concentration $N_c(\vec{r},t)$ ($c=e$ for electrons and $c=h$ for holes) at position $\vec{r}$ and time t of a three-dimensional valence system is given by

$$N_c(\vec{r},t)=\frac{2}{\sqrt{\pi}}Z_c(T^*)\int_0^\infty \frac{\sqrt{x}}{\exp\{x-\eta_c(\vec{r},t)\}+1}dx, \qquad (1)$$

where $Z_c(T^*)$ is the effective density of states at the effective temperature T^*, and η_c is the reduced quasi-Fermi-level, for electrons and holes, given by

$$\eta_e=\frac{\psi_e-E_C}{k_BT^*}, \quad \eta_h=\frac{E_V-\psi_h}{k_BT^*}. \qquad (2)$$

The symbols E_C and E_V represent the energies of the conduction-band minimum (CBM) and valence-band maximum (VBM), and k_B is the Boltzmann constant.

Based on the classical Boltzmann equation in the relaxation-time approximation for nonequilibrium thermodynamics, von Driel[24] has shown that the current $\vec{J}$ of pair concentration due to a strong Dember field (under the assumption $\vec{J}=\vec{J}_h=-\vec{J}_e$) is given by

$$\vec{J}=-D\left[\nabla N+\frac{N}{T^*}\left(\frac{\hat{B}}{\hat{A}}-\frac{3}{2}\right)\nabla T^*+\frac{N}{2kT^*}\frac{1}{\hat{A}}\nabla E_g\right], \qquad (3)$$

where $\hat{A}$ and $\hat{B}$ are Fermi-pressure factors,[24] given by

$$\hat{A}=\frac{F^e_{1/2}}{F^e_{-1/2}}+\frac{F^h_{1/2}}{F^h_{-1/2}}, \quad \hat{B}=\frac{F^e_1}{F^e_0}+\frac{F^h_1}{F^h_0}. \qquad (4)$$

Here, F^c_j denotes the Fermi-Dirac integral of order j for the carriers, and D designates the ambipolar diffusion constant for excess carriers defined by

$$D=\frac{2kT^*}{e_0}\frac{\mu_e\mu_h}{\mu_e+\mu_h}\hat{A}. \qquad (5)$$

The symbols μ_c and e_0 represent the carrier mobility and unit charge, respectively. Therefore, under dense-excitation conditions, the pair-concentration flow is governed by the density-dependent diffusion constant D, the concentration gradient, the temperature gradient, and the band-gap gradient ∇E_G.

In terms of $\vec{J}$ of Eq. (3), the local density of carriers is governed by the equation of particle balance, given by

$$\frac{\partial N(\vec{r},t)}{\partial t} + \nabla \cdot \vec{J} = G(\vec{r},t) - R(\vec{r},t), \tag{6}$$

where G and R are the pair generation and recombination rates.[24] By solving Eq. (6) under appropriate boundary conditions, we can evaluate the density of valence holes in the subsurface layer, which corresponds to the hole density in Sumi's theory for two-hole localization.

B. Rate of two-hole localization

First, we summarize briefly the rate of THL, for equilibrated electron-lattice systems, formulated by Sumi.[15] The rate J of surface bond rupture, due to successive two-hole localization, is given by

$$J = N_d R_{SHL}, \tag{7}$$

where N_d is the density of bonds localizing the first hole, and R_{SHL} is the rate constant for localizing a second hole at the same bond. For the first-hole localized metastable state with energy E_d (measured from the VBM), N_d is determined by the Fermi distribution function with Fermi energy E_F. In the case where E_d is larger than E_F, and in order to satisfy the condition, $\exp\{(E_d - E_F)/k_B T\} \gg 1$, N_d is approximated as

$$N_d = N_0 \exp\{-(E_d - E_F)/k_B T\}, \tag{8}$$

where N_0 represents the total density of bonds capable of holding the first localized hole. The rate constant R_{SHL} is approximated by

$$R_{SHL} \approx C \exp(E_F/k_B T). \tag{9}$$

The constant C is specific to the system under consideration and is defined as

$$C = [4\pi/(\hbar^2 S k_B T)]^{1/2} \int dE\, g(E) \times \exp[-E/k_B T - (E_b + U - E)^2/(4 S k_B T)]. \tag{10}$$

In Eq. (10), the function $g(E)$ is a spectral function of the matrix elements M_{fb}'s for the transitions from a delocalized state f (with energy E_f) to the two-hole localized state, and given by

$$g(E) = \sum_f |M_{fb}|^2 \delta(E - E_f). \tag{11}$$

Also, S represents the lattice-relaxation energy associated with the second-hole localization, U is the Coulomb repulsive energy between the two holes localized on a single bond, and E_b ($\sim B/2$) is the kinetic energy lost in the process of localizing the second hole at the bond, which is related to the valence band width B. All of these parameters are material and surface specific, and give the following energy relationship for neutral-atomic desorption due to bond rupture by THL:

$$E_b + U - S \leq 0. \tag{12}$$

Also, under the condition given by Eq. (8), the rate expression of Eq. (9) is valid when the average kinetic energy E_T of free holes, that tunnel most frequently to one of the first-hole localized bonds, satisfies the condition $E_F < E_T \ll U$.[15] Then, J is given by

$$J = N_0 C \exp(-E_d/k_B T)\exp(2E_F/k_B T). \tag{13}$$

As seen in Eq. (13), J depends on the excitation density through the factor $\exp(2E_F/k_B T)$.

For three-dimensional dense valence excitation associated with strong carrier diffusion, the Fermi energy is no longer the quantity that characterizes the hole distribution and dynamics. In this case, the quasi-Fermi-level ψ_h (or η_h) characterizes the hole distribution as shown in Sec. II A. Under the presumption of local equilibrium, the Fermi energy E_F, for equilibrated electronic systems, can be replaced by the quasi-Fermi-level of valence holes near the surface. Then, under the restriction $\psi_h < E_T \ll U$, Eq. (13) (valid for equilibrated valence holes) becomes

$$J = J_0 N_0 \exp[2\eta_h(0)], \tag{14}$$

valid for nonequilibrated valence holes, where J_0 is defined as

$$J_0 \equiv C \exp(-E_d/k_B T^*), \tag{15}$$

and $\eta_h(0)$ represents the reduced quasi-Fermi-level in the subsurface layer. When we take $N(0,t)$ of the solution of Eq. (6) as the local hole density of the subsurface layer, we can evaluate $\eta_h(0,t)$, based on the relation between $N(0,t)$ and $\eta_h(0,t)$ of Eq. (1), and determine J from Eq. (14).

Since there are no analytical expression of $F_{1/2}(\eta)$ in the general case, J cannot be expressed in an analytical form as a function of the hole density. However, for the case where $\eta_h(0)$ is smaller than 2, we can use Ehrenberg's expression for $F_{1/2}(\eta_h)$:

$$F_{1/2}(\eta) = \frac{2\sqrt{\pi}\exp(\eta)}{4 + \exp(\eta)}. \tag{16}$$

In this excitation density regime, the relation between hole density and the reduced quasi-Fermi-level simplifies and we can express J as

$$J = N_0 J_0 \left(\frac{Z_h}{N(0,t)} - 0.25\right)^{-2}. \tag{17}$$

In the case of Si, where $Z_h = 1.04 \times 10^{19}$ cm^{-3} at room temperature,[27] the above conventional expression may be valid for hole densities up to $\sim 2 \times 10^{19}$ cm^{-3}.

Although the theory predicted significant screening effects under dense excitation,[28] the excitation densities considered here are much smaller than the range considered in the theory. In fact, screening effects become appreciable only for densities greater than 5×10^{20} cm^{-3} in Si,[29] far above Z_h. Therefore, for excitation densities less than Z_h, we can neglect screening effects, and the expressions derived above are valid.

In Fig. 1, we present the calculated result of Eq. (17), as a function of the normalized hole density n_h ($=N(0)/Z_h$), and compare it with the result from the exact numerical solution of Eq. (14). It is clear that the approximate form for the THL rate is valid for n_h less than 1.8, and is applicable to the experimental results studied so far. This result also shows

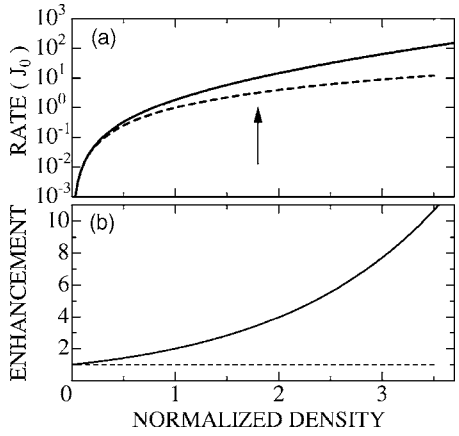

FIG. 1. The bond-rupture rate calculated as a function of normalized density $n_h(=N(0)/Z)$ of valence holes in the subsurface layer. The solid curve is the result of a numerical calculation of Eq. (12) and the gray curve is the result of the approximated form for moderate excitation density, Eq. (15). The broken curve represents the square of n_h. (b) Deviation of the calculated rate versus the square of n (in linear scale) showing the enhancement of the rate due to the quantum statistics of valence holes.

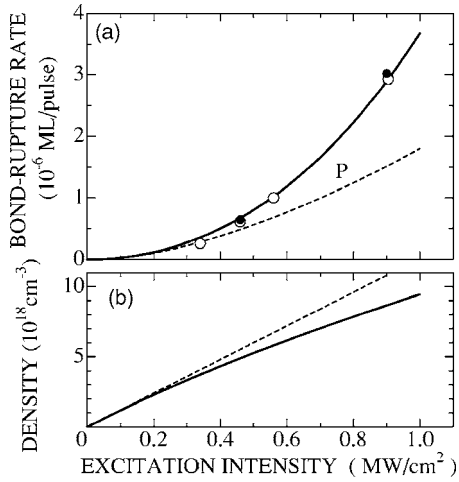

FIG. 2. (a) The rate of bond rupture of P atoms on InP(110)-(1×1) as a function of the excitation intensity as determined by the STM observation (●) and by desorption measurements (○) (Ref. 12). The solid curve is the calculated result of Eq. (15), while broken curve shows the quadratic rate dependence. (b) The maximum density of valence holes in the subsurface layer formed by a 5-ns laser pulse calculated using Eq. (6) under the boundary conditions of Eq. (16) with $S_R=1\times10^5$ cm/s. The other parameters are listed in the text. The broken line shows the linear relation between $N(0)$ and the excitation intensity.

that J deviates from the quadratic relation for a weak-excitation condition around $n_h\sim0.01$. The deviation, or the enhancement of J due to hole quantum statistics, is shown in Fig. 1(b) for comparison.

III. COMPARISON OF THE THEORY WITH EXPERIMENTAL RESULTS

As formulated above, Eq. (14) correlates the density of valence excitation and the absolute rate of bond rupture on surfaces. Therefore, to test the present theory, the absolute rate of bond rupture as a function of excitation density is highly desirable. Although several studies have reported relative laser desorption yields none give absolute rates. Furthermore, surface defects strongly influence desorbed species and their yields, making it difficult to assess the correlation between the theory and experimental quantitatively. Therefore, we focus on absolute rate results obtained by scanning tunneling microscopy (STM) observation, on well-characterized surfaces. Despite this restriction, there are sufficient ideal data for a statistically significant analysis including: P-bond rupture on InP(110)-(1×1) under visible ns-laser excitation and Si-bond rupture on Si(111)-(2×1) under infrared (1064-nm) ns-laser excitation.

A. *P*-bond rupture on InP(110)-(1×1)

Gotoh *et al.* have shown that the electronic bond rupture of P and In atoms on InP(110)-(1×1) can be induced under bulk-valence excitation at room temperature.[12] The rate of bond rupture is found to be super linear with excitation intensity I_{ex}, as is generally observed on semiconductor surfaces. As discussed in the Introduction, these surfaces have no intrinsic band-gap states. Also, the surfaces had low vacancy concentrations, less than 0.001 ML prior to excitation (hereafter we refer to surfaces with low defect concentrations as LDC surfaces). Defect-induced band bending is negligible in LDC surfaces.[30] Therefore, bulk valence excitation of LDC InP(110)-(1×1) shows three-dimensional features associated with strong concentration gradients and carrier flows. As a first test of the present theory, we analyze bond breaking processes of P atoms on InP(110)-(1×1) LDC surfaces.

Figure 2 displays the rate of P-bond rupture per pulse as a function of excitation intensity, I_{ex}, of 2.65-eV photons. The rate is given in terms of ML/pulse, by setting $N_0=1$. (We use these units hereafter.) The open and solid circles show previously reported results from P-atomic desorption and STM imaging measurements, respectively.[12] Although desorption results were obtained on a relative scale, quantitative correlation between STM and desorption results makes it possible to determine the absolute rate of bond rupture. Figure 2 shows clearly that the bond-rupture rate depends superlinearly on the excitation intensity. The solid curve is the result of theoretical analysis obtained by the method described below.

In a theoretical calculation of J, we first solve numerically the particle balance equation for $N(0,t)$. Laser-induced heating, estimated from standard formulas,[31] is at most 30 K even for the highest excitation intensity used,[12] and we can neglect temperature gradient effects in Eq. (3). As shown by Eq. (5), D depends on the density through the Fermi-pressure factor $\hat{A}$. However, $\hat{A}$ becomes only ~20% larger than the low-density limit value of unity, even for the density equal to Z_h, corresponding to $\exp(\eta_h)\approx2$. Since this effect is small in the present excitation density range, we also neglect the density dependence of D. Similarly, we can also neglect the band-gap gradient dependence for densities less than Z_h [Eq.

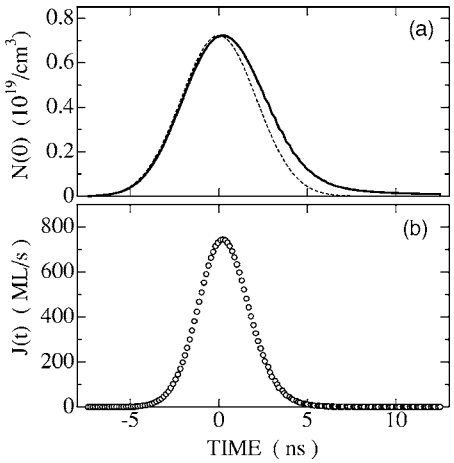

FIG. 3. (a) Calculated valence hole density $N(0,t)$ in the subsurface layer generated by a 5-ns laser pulse as a function of time (solid line). The broken curve shows the laser-pulse shape. (b) Calculated bond-rupture rate as a function of time using Eq. (15) with constant value $J_0=2.4\times10^2$ s^{-1}.

(3)]. Therefore, the equation of particle balance can be reduced to a normal one-dimensional diffusion equation along the distance z (in unit of cm) from the surface in this case. We use the standard boundary conditions:[23]

$$N(z\rightarrow\infty,t)=N_h^0,\quad \left(D\frac{\partial N}{\partial z}\right)_{z=0}=S_R N(0,t), \tag{18}$$

where N_h^0 is the concentration of holes under equilibrium conditions, and S_R is the surface recombination velocity. For the n-type specimens used in the experiment, the majority carrier (electron) concentration is 4.5×10^{15} cm^{-3}.[12] Therefore, N_h^0 is effectively set to zero. In the calculation of Eq. (6), S_R was treated as an unknown, since its magnitude has not yet been determined for such LDC surfaces. To calculate $N(0,t)$ we use the absorption coefficient and reflectivity at 460 nm from Ref. 32, the radiative-recombination rate of 1.2×10^{-10} cm^3 s^{-1}, and the Auger recombination rate of 9×10^{-31} cm^6 s^{-1}.[33]

In Fig. 3(a), we show the result of $N(0,t)$ thus determined as a function of time for $I_{ex}=0.9$ MW cm^{-2}. Based on this result, we evaluated $\eta_h(0,t)$ as a function of time using the effective valance hole density of $Z_h\approx1\times10^{19}$ cm^{-3}. The maximum value of ψ_h $[=k_BT\eta_h(0)]$ for the highest excitation intensity is +0.03 eV, which is considerably less than the calculated value of E_T (=0.13 eV) and U (=0.83 eV) for InP(110)-(1×1).[34] Therefore, Eq. (13) can be applied for the present analysis. Also, since the maximum value of $N(0,t)$ is less than $2Z_h$ for the highest excitation intensity, we can use the approximated form of $J$of Eq. (17) to calculate the bond-rupture rate $J(t)$. The result of $J(t)$ for $I_{ex}=0.9$ MW cm^{-2}, at constant J_0, is shown in Fig. 3(b). Since the experimental results in Fig. 2(a) are obtained as the rate per pulse, we integrated $J(t)$ with respect to time to evaluate the bond-rupture rate $K(I_{ex})$ per pulse for a given intensity I_{ex}. The calculated results of $K(I_{ex})$ are shown by the solid curve in Fig. 2(a). In the figure, it is clear that the calculated $K(I_{ex})$ is

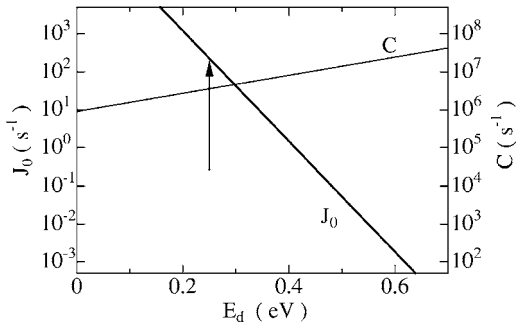

FIG. 4. The calculated value of J_0 (left scale), and C (right scale), of Eq. (15) as a function of E_d. The arrow shows the magnitude of E_d corresponding to the best-fit value of J_0 in Fig. 2.

superlinear with respect to I_{ex}, and can reproduce the experimental results obtained for InP LDC surfaces.

To examine the superlinear nature of $K(I_{ex})$ further, we calculated the maximum value of $N(0,t)$ as a function of I_{ex}. As seen in Fig. 2(b), the density tends to saturate at higher excitation intensities due to effective radiative recombination in this crystal. It is evident that the bond-rupture rate depends more strongly on I_{ex} than the square of n_h [see Fig. 2(a)]. The stronger dependence is due to a quantum statistical effect of the dense valence hole distribution as expressed by the factor $\exp\{2\eta_h(0)\}$.

In the evaluation of $K(I_{ex})$, we assumed $J_0=2.4\times10^2$ s^{-1} as fit from the absolute magnitude of the STM results. Since the quantity $J_0[=C\exp(-E_d/kT)]$ is the factor to determine the absolute magnitude of the rate, quantitative examination of this constant provides an additional test of the theory.

The magnitude of C for P-bond rupture on InP(110)-(1×1) can be calculated using Eq. (10) by inputting energy values, most of which are obtainable from published data.[15,34] In Fig. 4, we plot the calculated value of J_0 as a function of E_d. The dependence is mainly determined by the exponential term of E_d, although the magnitude of C varies somewhat with E_d. For InP(110)-(1×1), the first hole is localized to form a metastable state on the highest occupied surface state (S_1) composed of s-like dangling bonds of anion atoms. The electronic structure of S_1 has been characterized by photoelectron spectroscopy.[35,36] The S_1 state is located 0.2 eV below the VBM at the $\bar{\Gamma}$ point of the surface Brillouin zone, and shows a dispersion width of about 0.8 eV. Therefore, we can take the average energy of 0.6 eV to be the level of the localized state. However, the energy of E_d is less than the average energy because the lattice relaxes upon hole localization. Although the lattice relaxation energy is not reported for hole (or electron) localization on surfaces, one may expect an energy of about 0.3 eV.[15] Additionally, an enhanced ionicity of the surface bonds, due to a net charge transfer from In to P atoms in the (1×1) surface structure, may lead to a larger lattice relaxation energy upon carrier localization from significant optical-phonon contributions.[37] The plot of J_0 in Fig. 4 shows that the E_d, corresponding to $J_0=2.4\times10^2$ s^{-1}, is about 0.25 eV, which suggests a lattice relaxation energy of 0.35 eV. As discussed above, this is a highly likely energy for the hole-localized surface state. Therefore, the present theory reasonably describes not only

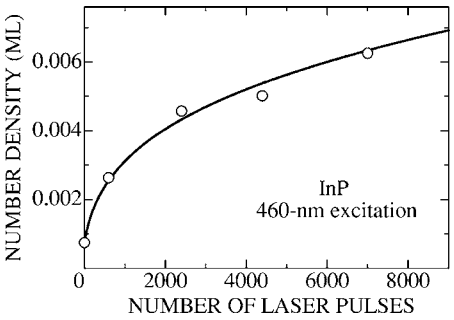

FIG. 5. Total number density of surface vacancies versus number of incident laser pulses (after Ref. 12). The solid curve is the calculated bond-rupture rate as a function of the surface-vacancy concentration (see text for details).

the superlinear dependence of the bond-rupture rate on I_{ex}, but also its absolute magnitude.

In order to examine the validity of the present theory further, we analyze the bond-rupture rate as a function of surface-defect concentration. In a previous STM study of P-atom desorption from laser-excited InP surfaces, it was shown that the rate of surface bond rupture depends on the concentration of surface vacancy sites.[12] On *n*-type InP surfaces, P vacancies are charged negatively[38] such that they interact effectively with valence holes. Therefore, a precise analysis of the effects of surface vacancies may provide a crucial test for the present theory. On damaged surfaces, bond rupture at originally perfect sites and at sites near preexisting defect sites takes place within the same exciting laser pulse.[12] In order to simplify the analysis, the number density N_j and vacancy-site density V_j of a surface vacancy cluster consisting of j vacancy sites was introduced.[12] The number density N_j is registered simply as a count of vacancy clusters irrespective of their size. The site density V_j is registered as j, the number of sites in an individual vacancy cluster. Any bond ruptures at sites nearest preexisting vacancies enhance the total vacancy-site density V $(=\Sigma_j V_j)$, but do not change the total number density N $(=\Sigma_j N_j)$. Therefore, N represents the concentration of vacancies newly formed at originally perfect sites free from vacancy formation near preexisting defect sites. In Fig. 5, we show N as a function of the number of incident laser pulses.[12] From the plot, we can evaluate the rate of bond rupture from the slope of N. An initial observed slope of 3×10^{-6} ML/pulse reduces to a slope of 2.3×10^{-7} ML/pulse after 7000 pulses, where the total surface-vacancy site density (V) increases to a maximum of 0.034 ML. Since the reduction in N_0 of Eq. (14) is negligible for $V=0.034$ ML, it is clear that the factor $\exp(2\eta_h)$ decreases sharply with increasing defect concentration. In view of the effective interaction between valence holes and negatively charged surface vacancies, it is possible that hole localization around pre-existing P vacancies may serve to enhance bond breaking near defects. Such an effect would lead to a efficient formation of vacancy clusters as observed experimentally.[39] On the other hand, defect-assisted hole localization reduces the density of valence holes in the near surface region. Because the factor $\exp(2\eta_h)$ is strongly dependent on $N(0)$, a small reduction of $N(0)$ could significantly decrease the magnitude of the bond rupture rate K. Therefore, the result in Fig. 5 is qualitatively consistent with the THL mechanism.

Hole trapping by pre-existing vacancies can be treated by introducing a vacancy-concentration dependent term in S_R, for damaged surfaces,

$$S_R(V) = S_0 + \sigma V. \tag{19}$$

The symbol σ represents the average trapping velocity per surface vacancy. In principle, the trapping velocity may depend on the size and form of vacancy clusters. However, we assumed in Eq. (19) that each vacancy site has the same average trapping velocity, characterized by σ, since the dependence of the trapping velocity on surface-vacancy size (and form) is not yet known. Based on the experimentally determined total vacancy-site densities V, we solve Eq. (6) with the $S_R(V)$ to have $N(0,t)$ for the surfaces with a given surface vacancy concentration. Then, the bond rupture rate per pulse (K) is evaluated, similar to the case of LDC surfaces. The result is shown by the solid curve in Fig. 5; it can describe reasonably the growth curve of N, or, the bond-rupture rate K as a function of V. The magnitude of σ obtained by the fitting procedure is 3.7×10^{-8} cm^3 s^{-1}, which is larger, by more than a factor of 100, than the magnitude of S_0/N_0 $(2\times10^{-10}$ cm^3 s$^{-1})$ for a perfect surface. The large value may partly reflect an effective interaction between valence holes and surface-vacancy clusters. Thus, the present theory of THL can reproduce the experimental results of excitation-induced bond breaking on InP(110)-(1×1) not only qualitatively, but also quantitatively.

B. Si-bond rupture on Si(111)-(2×1)

The Si(111)-(2×1) surface is characterized by quasi-one-dimensional zigzag chains of Si atoms associated with a substantial buckling. The buckling is accompanied by a net charge transfer from down (Si_{down}) to up (Si_{up}) atoms that induces a significant ionicity in the bonding.[1] It has been shown that Si_{up} atoms, at intrinsic sites, are subject to electronic bond rupture under valence excitation with 1.16 eV photons that induce the lowest indirect band-gap excitation with an excess energy of only 0.04 eV (the band-gap energy of Si at 300 K is 1.12 eV).[11] Figure 6 shows the rate of bond rupture at perfect surface sites that again displays a superlinear dependence on the excitation intensity. Based on the known magnitudes of linear and two-photon absorption coefficients,[24] it has been shown that the one-photon valence excitation is exclusively responsible for the electron-hole generation in the excitation-intensity range in Fig. 6.[11] Silicon has an extremely small absorption coefficient $(\sim11$ cm$^{-1})$ (Ref. 24) at 1.16 eV such that optical excitation should be almost uniform and carrier diffusion from the surface to the bulk negligible. However, fast surface recombination[21] can induce a density gradient in the valence-hole concentration leading to net transport from the bulk to the surface. This process could enhance surface-bond breaking. Analysis of experimental desorption results on Si(111)-(2×1) can, therefore, provide another test of our theory.

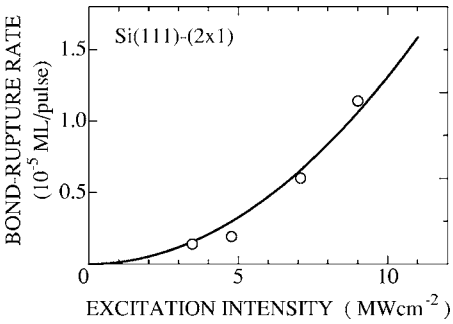

FIG. 6. The rate of bond rupture of Si atoms on Si(111)-(2×1) determined by the STM observation of irradiated surfaces as a function of the excitation intensity (after Ref. 11). The solid curve is the calculated result of Eq. (17) using a surface recombination velocity of 5×10^4 cm/s.

Before analyzing the results, we briefly discuss possible effects of band bending on hole dynamics. The Fermi level of the *n*-type surface is pinned 0.38±0.1 eV above the VBM (Ref. 1) leading to an upward bending and an accumulation of photogenerated holes in the surface region. This initial accumulation of surface valence holes may explain the enhanced yield of surface-vacancy formation observed for *n*-type surfaces.[11] However, as demonstrated by two-photon photoemission spectroscopy,[21] under intense excitation, the band becomes flattened due to photovoltaic effects.[1] The band flattening occurs rapidly, within a few ps of excitation. Therefore, under ns-laser excitation, most photogenerated carriers are subject to flat-band conditions and the present theory should apply.

To evaluate the role of bulk to surface hole diffusion, we solved the equation of particle balance numerically using similar boundary conditions as used for InP. We used reported values for the absorption coefficient (11 cm^{-1}), reflectivity (0.30), ambipolar diffusion constant (18 cm^2 s^{-1}), Auger recombination coefficient (3.8×10^{-31} cm^3 s^{-1}) (Refs. 24 and 33) and treated the surface recombination velocity as an unknown parameter. In Fig. 7(a), we plot the hole density at the surface as a function of time for 3.5-ns pulse excitation at I_{ex}=9.1 MW cm^{-2}. Because of slow Si carrier decay rates, the density at the surface can reach $\sim10^{18}$ cm^{-3} at the end of the highest intensity 3.5-ns pulses. The gradual decay of $N(0,t)$ results from the slow decay rates and from persistent hole diffusion from the bulk to the surface. Since the maximum density calculated is smaller than Z_h, Eq. (17) is applicable. Figure 7(b) shows the bond-rupture rate $J(t)$ evaluated from the result of $N(0,t)$. The bond breaking process induced by a 3.5-ns laser pulse lasts effectively for a few tens of ns. Then, by integrating $J(t)$ with respect to time, we evaluated the bond-rupture rate K per pulse for this excitation intensity. The result of K calculated as a function of the excitation intensity is plotted (the solid curve) in Fig. 6. Again, the calculated results fit the experimental data reasonably well.

In order to fit the simulated results to the experimentally determined absolute value of K, we used the values $J_0=3.5\times10^4$ s^{-1} and $S_R=5\times10^4$ cm s^{-1}. We did not try to obtain the best fit, since a rather wide range of S_R (from 5×10^3 cm s^{-1} to 8×10^4 cm s^{-1}) gave a similar non-

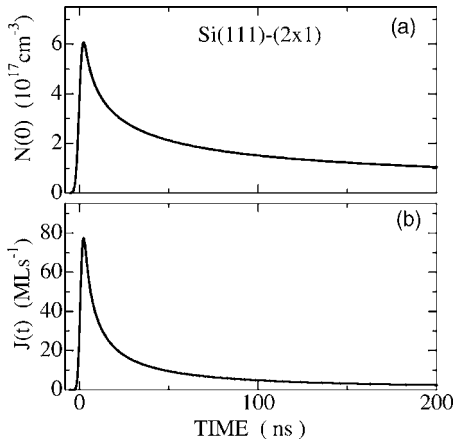

FIG. 7. (a) Calculated valence hole density $N(0,t)$ in the subsurface layer generated by a 3.5-ns laser pulse as a function of time. (b) Calculated bond-rupture rate as a function of time. In this calculation, Eq. (17) was used with $J_0=3.5\times10^4$ s^{-1}.

linear dependence. On this surface, the surface π band localizes valence holes to form the first-hole localized state. The surface π band is in near degeneracy with the VBM[1] and we assume that E_d=0. Even in this case, we can still use the formula of Eq. (8), since $\eta_h\leq-5$ for the present range of hole densities and $\exp(-\eta_h)\gg1$. The value of C calculated using literature data[1,27] is 5×10^4 s^{-1}, which is consistent with the parameter used in Fig. 6.

The surface recombination velocity used in the calculation is 5×10^4 cm s^{-1}, much smaller than the value of 3×10^7 cm s^{-1} evaluated for an *n*-type surface at the low-injection limit.[21] Halas and Bokor have pointed out the important role of the time-dependent surface photovoltage shift that governs surface recombination in the subnanosecond temporal domain on this surface.[21] This photovoltage shift should be taken into account if a more detailed analysis of short-time valence hole localization is required as in the case of fs-laser excitation. From this point of view, in terms of a one parameter surface recombination velocity, our present calculation may be too simple to describe the dynamics fully. However, the temporal width of our laser pulse is 3.5 ns and bond-breaking processes last for a few tens of ns as shown in Fig. 7. Therefore, we may take the value as an overall average of the surface recombination velocity, in the nanosecond regime, for valence hole relaxation under flat-band conditions.

IV. SUMMARY

We have extended the THL model, originally formulated by Sumi, to treat nonequilibrium three-dimensional valence hole distributions. We find that the quasi-Fermi-level plays an important role in modeling the rate of two-hole localization, and hence the bond-rupture rate of atoms at intrinsic surface sites. The particle balance equation, solved numerically with appropriate boundary conditions, gives the valence-hole density in the near surface region, which is the key quantity necessary to calculate the per pulse bond-rupture rate. We then applied the extended model to analyze

photoinduced structural instability on InP(110)-(1×1) and Si(111)-(2×1) surfaces and conclude that the THL model can be applied generally to predict rates of laser-induced bond ruptures on semiconductor surfaces. The present theory successfully describes experimental results not only on surfaces with low defect concentrations, but also on surfaces where the interaction between valence holes and surface defects is significant. Future development based on first principles theoretical modeling of short-time carrier dynamics should provide further insight into surface-specific behavior of semiconductors.

ACKNOWLEDGMENTS

The authors are grateful to H. Sumi for valuable comments and stimulating discussions. This work was supported by a Grant-in-Aid for Scientific Research from the Ministry of Education, Science, Technology, Sports, and Culture of Japan. W.H. thanks the US Department of Energy, Office of Science, Division of Chemical Sciences, and the Environmental Molecular Sciences Laboratory operated by the Office of Biological and Environmental Research at PNNL for support.

[1] W. Mönch, *Semiconductor Surfaces and Interfaces* (Springer, Berlin, 1995).
[2] J. P. Long, S. S. Goldenberg, and M. N. Kabler, Phys. Rev. Lett. **68**, 1014 (1992).
[3] K. Ishikawa, J. Kanasaki, K. Tanimura, and Y. Nakai, Solid State Commun. **98**, 913 (1996).
[4] J. Xu, S. H. Overbury, and J. F. Wendelken, Phys. Rev. B **53**, R4245 (1996).
[5] X. H. Chen, J. C. Polanyi, and D. Rogers, Surf. Sci. **376**, 77 (1997).
[6] J. Kansaki, T. Ishida, K. Ishikawa, and K. Tanimura, Phys. Rev. Lett. **80**, 4080 (1998).
[7] J. Kanasaki, K. Iwata, and K. Tanimura, Phys. Rev. Lett. **82**, 644 (1999).
[8] B. Y. Han, K. Nakayama, and J. H. Weaver, Phys. Rev. B **60**, 13846 (1999).
[9] H. Kwak, K. C. Chou, J. Guo, and H. W. K. Tom, Phys. Rev. Lett. **83**, 3745 (1999).
[10] J. Kanasaki, M. Nakamura, K. Ishikawa, and K. Tanimura, Phys. Rev. Lett. **89**, 257601 (2002).
[11] E. Inami, K. Ishikawa, and K. Tanimura, Surf. Sci. Lett. **540**, L587 (2003).
[12] T. Goto, S. Kotake, K. Ishikawa, J. Kanasaki, and K. Tanimura, Phys. Rev. Lett. **93**, 117401 (2004).
[13] G. Chiarotti, S. Nannarone, R. Pastore, and P. Chiaradia, Phys. Rev. B **4**, 3398 (1971).
[14] S. Tanaka and K. Tanimura, Surf. Sci. **529**, L251 (2003).
[15] H. Sumi, Surf. Sci. **248**, 382 (1991).
[16] D. E. Ramaker, C. T. White, and J. S. Murday, Phys. Lett. **89A**, 211 (1982).
[17] A. Yasui, T. Uozumi, and Y. Kayanuma, Phys. Rev. B **72**, 205335 (2005).
[18] N. Itoh and T. Nakayama, Phys. Lett. **92A**, 471 (1982).
[19] P. W. Anderson, Phys. Rev. Lett. **34**, 953 (1975).
[20] M. Weinelt, M. Kutschera, R. Schmidt, C. Orth, T. Fauster, and M. Rohlfing, Appl. Phys. A **80**, 995 (2005).
[21] N. J. Halas and J. Bokor, Phys. Rev. Lett. **62**, 1679 (1989).
[22] J. P. Long, H. R. Sadeghi, J. C. Rife, and M. N. Kabler, Phys. Rev. Lett. **64**, 1158 (1990).
[23] J. S. Preston and H. M. van Driel, Phys. Rev. B **30**, 1950 (1984).
[24] H. M. van Driel, Phys. Rev. B **35**, 8166 (1987).
[25] J. R. Goldman and J. A. Prybyla, Phys. Rev. Lett. **72**, 1364 (1994).
[26] S. Jeong and J. Bokor, Phys. Rev. B **59**, 4943 (1999).
[27] *Physics and Technology of Semiconductor Device*, edited by A. S. Grove (John Wiley and Sons, Inc., New York, 1967).
[28] E. J. Yoffa, Phys. Rev. B **21**, 2415 (1980); , **23**, 1909 (1981).
[29] T. Sjodin, H. Petek, and H. L. Dai, Phys. Rev. Lett. **81**, 5664 (1998).
[30] Ph. Ebert, K. Urban, L. Aballe, C. H. Chen, K. Horn, G. Schwartz, J. Neugebauer, and M. Scheffler, Phys. Rev. Lett. **84**, 5816 (2000).
[31] *Laser Annealing of Semiconductors*, edited by J. M. Poate and J. W. Mayer (Academic, New York, 1982).
[32] D. E. Aspnes and A. A. Studna, Phys. Rev. B **27**, 985 (1983).
[33] These recombination parameters and the valence band effective density of states for InP were taken from the Electronic archive of The Ioffe physico-technical institute on "New Semiconductor Materials: Characteristics and Properties" (http://www.ioffe.rssi.ru/SVA/NSM/).
[34] K. Tanimura, Phys. Rev. B **69**, 033301 (2004).
[35] L. Sorba, V. Hinkel, H. U. Middelmann, and K. Horn, Phys. Rev. B **36**, 8075 (1987).
[36] H. Qu, J. Kanski, and P. O. Nilsson, Surf. Sci. **255**, 237 (1991).
[37] M. Ueta, H. Kanzaki, K. Kobayashi, Y. Toyozawa, and E. Hanamura, *Excitonic Processes in Solids*, Springer Series in Solid-State Science Vol. 60 (Springer, Berlin, 1986), Chap. 4.
[38] Ph. Ebert, K. Urban, and M. G. Lagally, Phys. Rev. Lett. **72**, 840 (1994).
[39] J. Kanasaki, T. Gotoh, E. Inami, K. Ishikawa, and K. Tanimura (unpublished).